Biosensors and Bioelectronics xxx (xxxx) xxx

Contents lists available at ScienceDirect

Biosensors and Bioelectronics

journal homepage: www.elsevier.com/locate/bios

# Exploring a CRISPR/Cas12a-powered impedimetric biosensor for amplification-free detection of a pathogenic bacterial DNA☆

Dagwin Wachholz Junior [a,b,*], Rafael Gonçalves Pontes [a,b], Bruna M. Hryniewicz [a,b], Lauro Tatsuo Kubota [a,b]

[a] Institute of Chemistry, University of Campinas – UNICAMP, 13083-970, Campinas, Brazil
[b] National Institute of Science and Technology in Bioanalytic (INCTBio), Campinas, Brazil

ARTICLE INFO

*Keywords:*
CRISPR
Impedance biosensor
Label-free
PAM sequence
*S. aureus*
Sepsis

ABSTRACT

Timely and precise detection of bacterial infections is essential for improving patient outcomes and reducing healthcare costs, especially for sepsis, where delayed diagnosis increases mortality. Traditional culture- and PCR-based methods are time consuming and require complex sample processing, making them unsuitable for rapid diagnostics in resource-limited settings. CRISPR/Cas-based methods, particularly when combined with electrochemical sensing, offer a promising alternative for rapid point-of-care (POC) diagnostics of bacterial infections due to their simplicity and specificity. This study proposes a label-free impedimetric biosensor using the CRISPR/Cas12a system for rapid and amplification-free detection of *Staphylococcus aureus* DNA, a primary pathogen responsible for sepsis. By leveraging CRISPR/Cas12a's target-activated collateral cleavage on non-specific DNA reporters we investigated the impact of using a protospacer adjacent motif (PAM) sequence on detection sensitivity and specificity. Our biosensor demonstrated ultra-sensitive detection, with limit of detection as low as 20 aM for dsDNA targets in buffer and without any pre-amplification steps. The study also confirmed CRISPR specificity's dependence on the PAM sequence, showing that mismatches on targeting sequences reduces cleavage efficiency, with a drastic reduction in trans-cleavage activity for single mismatch in PAM-containing sequences. Additionally, we examined how the DNA reporter affects performance, noting reduced cleavage efficiency when a ssDNA target was paired with a dsDNA reporter. Furthermore, validation experiments using human serum samples confirmed the biosensor's accuracy for bacterial DNA detection in clinical settings. This work advances CRISPR-powered electrochemical biosensors, providing a detailed discussion on developing a highly sensitive, fast and amplification-free tool for early detection of sepsis-causing bacteria.

## 1. Introduction

The rapid and accurate pathogen identification in infections offers substantial clinical and economic benefits by preventing the widespread of the disease and reducing mortality (Caliendo et al., 2013; Pliakos et al., 2018). Bacterial infections, such as severe sepsis, pose an additional and growing healthcare challenge due to their rapid progression, which can lead to organ failure and death if not diagnosed and treated promptly (Mancini et al., 2010; Zasowski et al., 2016). Delayed recognition and treatment of sepsis are associated to significantly higher rates of morbidity and mortality, with more than 7 million deaths each year, making bacterial infections the second largest cause of death globally (Ikuta et al., 2022; Zasowski et al., 2016). A key factor contributing to delayed sepsis diagnosis is the reliance on culture-dependent methods for detecting bacteremia, often requiring 24–72 h to provide results (Bloos, 2015; Mancini et al., 2010). These assays require labor-intensive procedures, such as plating and bacteria cultivation; and trained personnel, making them unsuitable for rapid diagnostics. While molecular methods, like polymerase chain reaction (PCR)-based methods, can accelerate the identification of pathogenic organisms, they still involve complex sample preparation, specialized equipment, and are expensive, limiting their widespread use (Bloos, 2015; Deroco et al., 2021; Deroco et al., 2022; Mancini et al., 2010).

Electrochemical biosensors present a promising alternative for detecting bacteria-caused infections, resulting in improved patient outcomes and significantly decreasing hospital-associated costs (Deroco

☆ This paper is dedicated to the memory of Professor Lauro Tatsuo Kubota.

* Corresponding author. Institute of Chemistry, University of Campinas – UNICAMP, 13083-970, Campinas, Brazil.
*E-mail address:* d262814@dac.unicamp.br (D. Wachholz Junior).

https://doi.org/10.1016/j.bios.2025.117607
Received 17 December 2024; Received in revised form 30 April 2025; Accepted 18 May 2025
0956-5663/© 2025 Elsevier B.V. All rights are reserved, including those for text and data mining, AI training, and similar technologies.

et al., 2021; Kabay et al., 2022; Vidic and Manzano, 2021). These sensors offer simplicity and the potential to develop point-of-care (POC) devices, which are particularly valuable for use in resource-limited and decentralized settings (da Silva et al., 2017; Drain et al., 2014; Wu et al., 2023). These sensors operate by converting biological recognition events into measurable electrical signals, offering rapid and sensitive detection, often within minutes, making them highly attractive for applications where time is critical. Moreover, the inherent simplicity of these sensors allows for miniaturization, enabling the development of more compact and portable devices (da Silva et al., 2017; Deroco et al., 2023; Wu et al., 2023). In addition to being user-friendly, electrochemical biosensors are typically more cost-effective compared to conventional molecular methods, as they require fewer reagents, do not necessitate expensive equipment, and can be produced at large-scale using relatively inexpensive materials (da Silva et al., 2017; Deroco et al., 2023; Panicker et al., 2024). Despite their potential, one of the challenges with electrochemical sensors lies in their specificity, which may not provide the precision required for sepsis detection across diverse bacterial strains and infection sources in complex biological samples (Dai and Liu, 2019; Deroco et al., 2021).

To address these specificity limitations, the combination of electrochemical sensing with CRISPR technology has emerged as a powerful approach for diagnostics (Tang et al., 2021; van Dongen et al., 2020; Wachholz Junior and Kubota, 2024). CRISPR/Cas systems were originally discovered as a vital component of bacteria and archaea adaptive immune systems, detecting foreign nucleic acids based on their sequence and eliminating them through the endonuclease activity associated with a CRISPR-associated protein (Cas) (Barrangou et al., 2007; Chen and Doudna, 2017; Jinek et al., 2012). While different CRISPR endonucleases exist, they share a common reliance on a guide RNA (crRNA), which guides the Cas proteins to specifically recognize and cleave the targeting nucleic acid. This specificity is critical in sepsis diagnostics, where the ability to accurately and timely identify the pathogen responsible for the infection can guide treatment decisions. CRISPR-based diagnostic systems, particularly those employing Cas12a enzymes, offer additional target sequence-specific recognition, followed by collateral cleavage of non-specific nucleic acid reporters (Chen et al., 2018; Kaminski et al., 2021; Li et al., 2018; Li et al., 2019). This trans-cleavage activity allows for highly specific detection of target sequences, making CRISPR-based systems an alternative to traditional detection methods (Gootenberg et al., 2018; Tang et al., 2021). In recent years, the ability to reprogram Cas systems by designing specific crRNA sequences to target virtually any nucleic acid sequence has become highly valuable for developing rapid and accurate detection platforms for viruses, bacteria, genetic mutations, and other biomolecules (Chakraborty et al., 2022; Kaminski et al., 2021; Shi et al., 2024; Tang et al., 2021; Wachholz Junior and Kubota, 2024; Zhang et al., 2022).

CRISPR-powered electrochemical sensors are gaining traction as a hybrid solution that combines the specificity of CRISPR technology with the simplicity of electrochemical detection. On one hand, electrochemical sensors provide a robust and real-time detection method, while on the other, the CRISPR/Cas system offers an ideal recognition tool with high specificity and programmability (van Dongen et al., 2020; Wachholz Junior and Kubota, 2024). Recently, the use of CRISPR-based electrochemical sensors using labelled DNA/RNA reporter sequences has been widely explored. However, label-free platforms offer several advantages over labelled ones, including reduced assay complexity, lower costs, and faster results (Rahn et al., 2023; Wachholz Junior and Kubota, 2024). In this article we propose the construction of an impedimetric biosensor using the CRISPR/Cas12a system for the detection of *S. aureus* DNA, a major infection-causing bacterium. The development of label-free CRISPR-based electrochemical assays is poorly explored in the literature, and certain factors affecting overall performance, such as length and nature of the DNA reporter sequences, are not studied in depth. This article explores the construction of an ultra-sensitive and amplification-free biosensor, discussing in detail the influence of CRISPR/Cas reaction conditions and the trans-cleavage activity on ss- and dsDNA reporter sequences. Moreover, by considering the Cas12a requirement for the protospacer adjacent motif (PAM) sequence, we evaluated the PAM-dependency on the detection capability by analyzing different target scenarios. This investigation was conducted to explore the influence on detection sensitivity and specificity for sepsis-causing bacteria, and the results obtained could broaden the scope of label-free CRISPR diagnostics to other pathogens. The proposed biosensor represents a simple and accurate diagnostic tool capable of detecting ultra-low concentration of infectious bacteria in serum samples in minutes, making it appropriate for early and on-site diagnostics of sepsis.

## 2. Materials and methods

This section includes details of chemicals, instruments, and experimental procedures. These corresponding contents are available in the Supplementary Material File (SI).

## 3. Results and discussion

### 3.1. Working principle of the label-free electrochemical biosensor and feasibility of the CRISPR/Cas12a system

The detection principle of the label-free electrochemical biosensor is shown in Fig. 1a. This method is based on the collateral cleavage of non-specific DNA reporter sequences promoted by the target-activated ribonucleoprotein (RNP) complex in the presence of *Staphylococcus aureus* bacteria DNA. This phenomenon leads to a change in the charge transfer resistance ($R_{ct}$) at the interface between the SH-ssDNA-modified electrode and the electrolyte after target recognition, which is measured by electrochemical impedance spectroscopy (EIS) in the presence of $[Fe(CN)_6]^{3-/4-}$ redox probe in solution. The Nyquist plots presented in Fig. 1b show a semicircle that reflects the electron transfer kinetics of the $[Fe(CN)_6]^{3-/4-}$ probe at the electrode surface, and an augment in its diameter indicates an increase in the $R_{ct}$. As depicted in Fig. 1b, the non-modified gold electrode (bare Au) showed a very small $R_{ct}$ value (134 ± 12 Ω, black curve), indicating a fast electron transfer process and a clean Au electrode surface. After the first modification step, when the SH-ssDNA reporter sequences were immobilized, a clear increase in $R_{ct}$ (12.0 ± 0.8 kΩ, red curve) was observed, as a result of the repulsion between the redox probe and the negatively-charged backbone of the DNA sequences. $R_{ct}$ value was further increased when the electrode was modified with 6-mercaptohexanol (MCH), to prevent non-specific DNA-Au interactions and to obtain a well-aligned DNA monolayer. This blocking step leads to a decrease in electron permeation to the electrode surface, and an increase in $R_{ct}$ (15.3 ± 0.9 kΩ, blue curve). In contrast, when the electrode was incubated with the target-activated CRISPR/Cas12a solution (1 nM of ssDNA target), an obvious decrease in $R_{ct}$ value was observed (13.5 ± 0.2 kΩ, pink curve), demonstrating the successful cleavage of non-specific DNA reporter sequences by the CRISPR system. Cyclic voltammetry (CV) measurements further confirmed these modification steps and the correct function of the biosensor. The results shown in Fig. 1C demonstrate a pair of well-defined and symmetric redox peaks ($\Delta Ep$ = 86 mV, $I_{pa}$ = 82 μA, black curve) for the bare Au electrode. After the modification steps, an increase in the peak potential separation and a decrease in peak current signals were observed for the ssDNA reporter ($\Delta Ep$ = 140 mV, $I_{pa}$ = 68 μA, red curve) and MCH ($\Delta Ep$ = 236 mV, $I_{pa}$ = 50 μA, blue curve), indicating a lower electron transfer kinetics. However, after the CRISPR/Cas12a reaction, an increase in peak current and a decrease in peak potential separation ($\Delta Ep$ = 203 mV, $I_{pa}$ = 58 μA, pink curve) were observed.

In this work, two different CRISPR/Cas systems were designed to evaluate the influence of the PAM sequence on biosensing performance. As seen in Table S1, the target sequences were a dsDNA sequence composed of a targeting strand (TS) and a non-targeting strand (NTS −

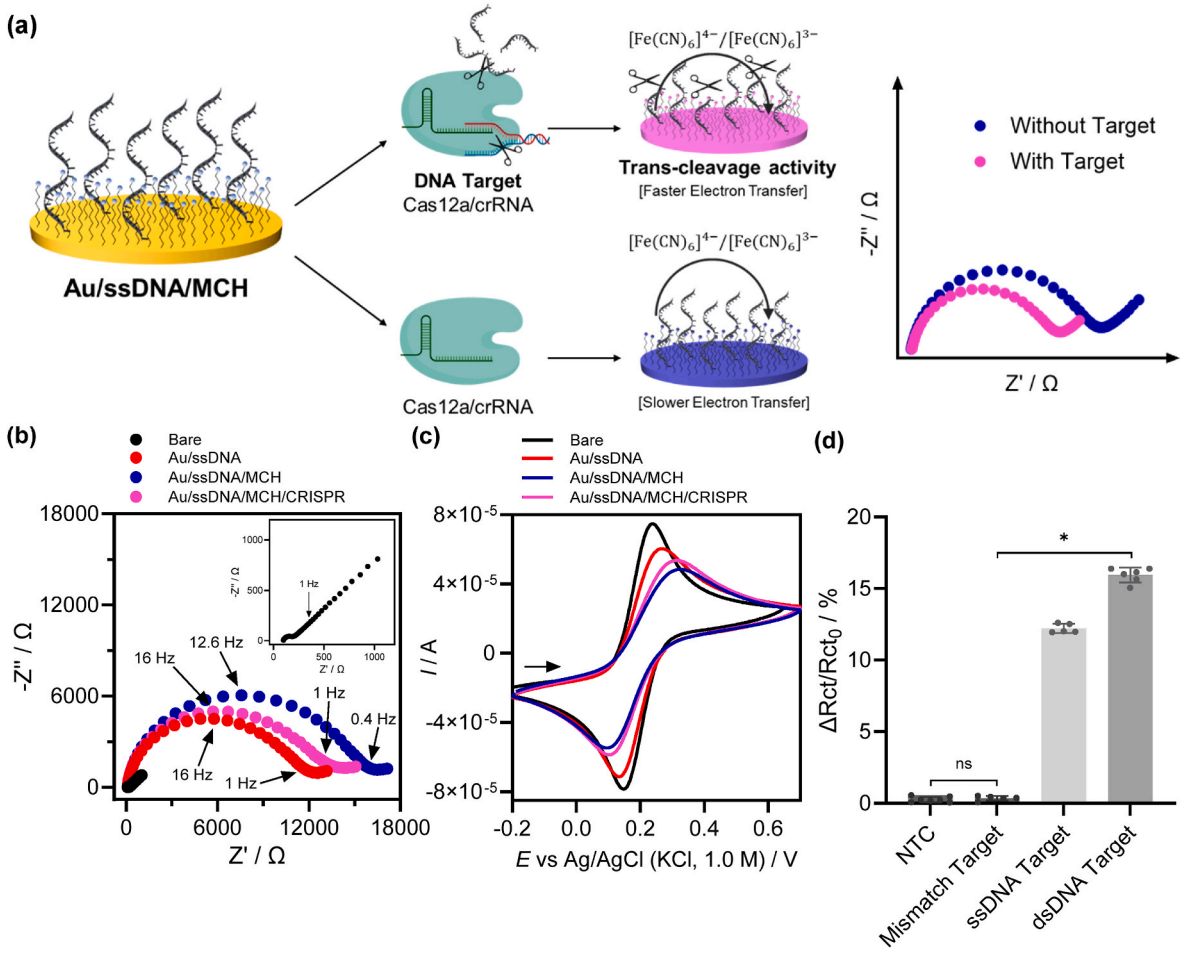



**Fig. 1.** **(a)** Schematic illustration of the working principle for label-free detection of *S. aureus* DNA by a CRISPR/Cas12a system; **(b)** Nyquist plots and **(c)** cyclic voltammograms for stepwise modification procedure: (**black** and inset) bare Au electrode, (**red**) Au/ssDNA, (**blue**) Au/ssDNA/MCH and (**pink**) biosensor after CRISPR/Cas12a reaction (Au/ssDNA/MCH/CRISPR); **(d)** Comparison of percentage of cleavage determined by the reduction in $R_{ct}$ ($\Delta R_{ct}/R_{ct0} \times 100$ %) after CRISPR reaction for different experimental conditions. All measurements were performed in measurement buffer (10 mM Tris-HCl, 100 mM NaCl, 10 mM $MgCl_2$, pH 7.4) containing 5 mM of $[Fe(CN)_6]^{3-/4-}$ redox probe. In all cases, 1 nM of target sequence and 50 nM of Cas12a/crRNA duplex were used. All data are expressed as mean ± standard deviation for $n \geq 5$ replicates. Statistical significance was analyzed using a two-tailed *t*-test: where ns = not significant with $p > 0.05$, and the asterisk (*) denotes significant differences with $\rho < 0.05$. (For interpretation of the references to colour in this figure legend, the reader is referred to the Web version of this article.)

which contains the PAM sequence) for the first scenario, and a ssDNA TS for the second one. For both scenarios, the same trans-cleavage activity experiments were conducted, and the feasibility of the two systems was further confirmed using polyacrylamide gel electrophoresis (PAGE) and EIS measurements. Fig. S1 shows that only in the presence of Cas12a/crRNA and target sequence, the CRISPR system is activated and cis- and trans-cleavage (lanes 6 and 7, respectively) are observed. In the absence of target sequence or if a mismatched target DNA sequence is used (lanes 5 and 8, respectively), no cleavage activity is noticed, neither for cis- or trans-cleavage. This is observed for both designed systems, with the Cas12a/crRNA duplex recognizing either the dsDNA (PAM-containing – Fig. S1(A)) and the ssDNA (PAM-absent – Fig. S1(B)) targets. The feasibility of the proposed system was also confirmed by EIS measurements. Fig. 1d shows that a reduction in $R_{ct}$ (or increase in the $\Delta R_{ct}$) value is only observed when a target-activated CRISPR system is used. When non-targeting control (NTC) or a non-complementary sequence is used, no collateral activity is observed, and the biosensor has no change in the electron transfer kinetics. With a fully complementary sequence, a clear change in $R_{ct}$ is noted, indicating a successful collateral activity. For both ssDNA and dsDNA targets, there is a decrease in $R_{ct}$ for 1 nM of target, but with lower collateral cleavage efficiency for the ssDNA target-activated system. This observation confirms the dependence on the target nature and will be explored in the next topics.

### 3.2. CRISPR/Cas12a reaction conditions optimization

Considering the trans-cleavage activity as critical for the overall biosensor performance, different reaction conditions were investigated. First, the activation time of the RNP complex was evaluated and it was observed that the CRISPR efficiency reached a maximum with 15 min of target activation, with both shorter and longer activation periods leading to decreased efficiency. The optimal 15-min activation time suggests that within this timeframe, the RNP complex undergoes crucial conformational changes and interactions required for efficient target recognition and cleavage. As seen in Fig. 2a, shorter periods (0 and 10 min) does not allow for the completion of these essential processes and may suffer from a diffusion-hindered process, once the entire recognition and cleavage steps occur in a confined space over the electrode. It is important to note that trans-cleavage does not occur at the same time as cis-cleavage (Chen et al., 2018). In contrast, longer activation times may introduce diminishing returns and potentially disrupt the RNP complex's functionality further impairing efficiency. Another important aspect is the Cas12a:crRNA ratio, once the precise stoichiometry is critical in RNA-guided systems. Fig. 2b shows that a maximum of

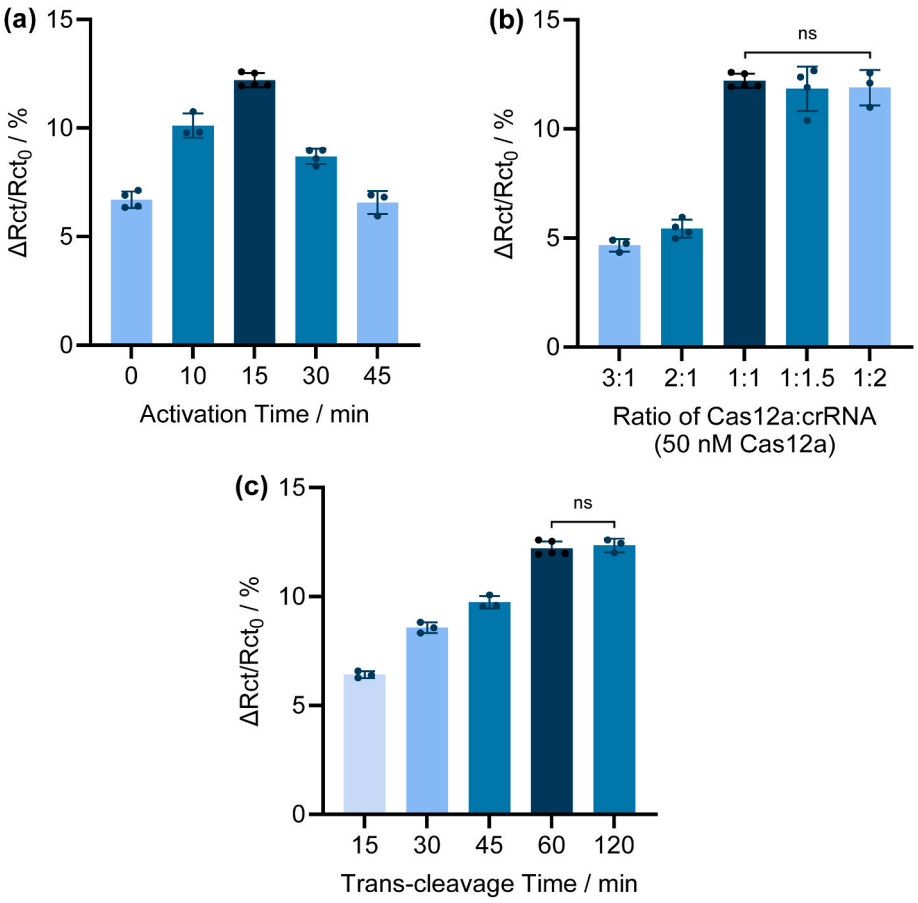



**Fig. 2.** Evaluation of the influence of the **(a)** activation time; **(b)** Cas12a:crRNA ratio; and **(c)** trans-cleavage period on the CRISPR/Cas12a reaction and biosensor performance. 1 nM of ssDNA target sequence and 50 nM of Cas12a/crRNA duplex were used (a and c). All data are expressed as mean ± standard deviation for n ≥ 3 replicates. Statistical significance was analyzed using a two-tailed *t*-test: where ns = not significant with ρ > 0.05.

trans-cleavage is reached when the same molar concentration of Cas12a and crRNA is used. This balanced stoichiometry ensures that each crRNA molecule is effectively loaded onto its respective Cas12a protein, thereby maximizing the efficiency of target recognition. For the 3:1 and 2:1 Cas12a:crRNA ratios, a drastic reduction in trans-cleavage efficiency is observed, related to a lower concentration of the activated duplex that effectively recognizes the target sequence. However, when the concentration of crRNA is increased (1:1.5 and 1:2) relative to the Cas12a enzyme, no change in cleavage efficiency is observed, as expected since the limiting factor in this case is the initial concentration of the

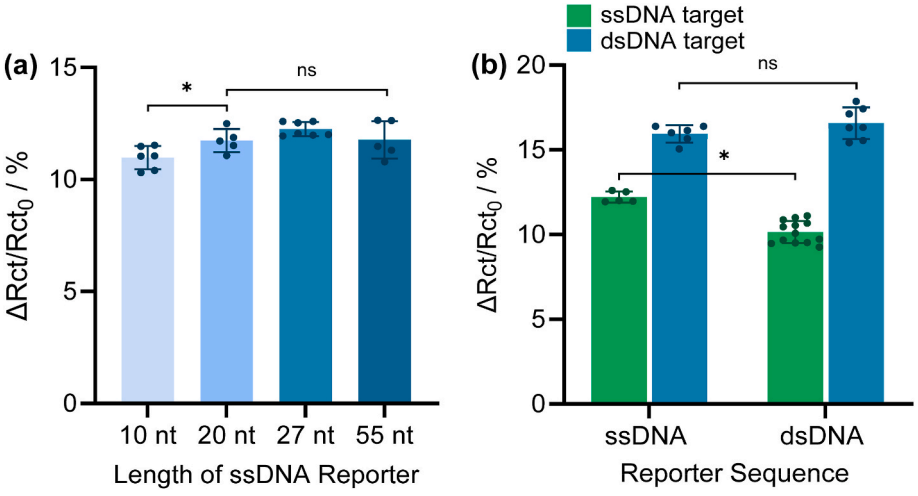



**Fig. 3.** Evaluation of the influence of **(a)** the ssDNA reporter length and **(b)** the nature of the DNA reporter (ssDNA or dsDNA) on the biosensor performance. In all cases, 1 nM of DNA target sequence and 50 nM of Cas12a/crRNA duplex were used. All data are expressed as mean ± standard deviation for n ≥ 5 replicates. Statistical significance was analyzed using a two-tailed *t*-test: where ns = not significant with ρ > 0.05, and the asterisk (*) denotes significant differences with ρ < 0.05.

endonuclease. Another experimental condition that influences the CRISPR collateral activity is the trans-cleavage time, and it was observed (Fig. 2c) that the collateral efficiency increased with larger incubation times, achieving a maximum after 1 h of trans-cleavage. The influence of reaction buffer, including buffer composition, NaCl and $Mg^{2+}$ concentration, pH and temperature during trans-cleavage are discussed in the SI.

### 3.3. Influence of the DNA reporter

In order to perform an efficient trans-cleavage step, the effect of the DNA reporter on the collateral cleavage efficiency is important. Optimization steps for the DNA reporter immobilization are discussed in the SI. Initially, different lengths of ssDNA reporter sequences were immobilized on the electrode surface, followed by the passivation with MCH molecules. As seen in Fig. S6, the $R_{ct}$ increased with the augment of the ssDNA length, once with longer ssDNA sequences, the electron tunneling distance to the electrode was increased, hampering the electron transfer kinetics. Furthermore, it can be observed in Fig. 3a, that an increase in the length of the ssDNA reporter leads to a vaguely increase in the collateral efficiency of the CRISPR system when the same concentration of ssDNA target is used. A significant difference can be observed ($\rho < 0.05$) when a 10 nt reporter sequence is used, leading to a lower detection efficiency. When a 20 nt sequence is immobilized, an increase in efficiency is observed (7 % higher than for 10 nt) leading to a maximum for 27 nt sequence. However, the difference between 27 nt and 20 nt produces only a minute variation (less than 5 %) which indicates a smaller dependence for longer reporters. This overall observation can be related to the formation of a more compact self-assembled monolayer for shorter ssDNA reporter sequences which can affect the diffusion and accessibility of the Cas12a endonuclease, further hindering its cleavage activity. By increasing the length of the ssDNA reporter, a flexible and accessible surface is created, promoting the approximation of the activated RNP complex. However, with further increase in sequence length, a slightly decrease in activity is observed, which can be associated with the higher malleability of longer ssDNA sequences that can fold over themselves creating a steric hindrance to the Cas12a enzyme. Furthermore, longer ssDNA sequences possess a higher signal-to-background ratio after CRISPR reaction, and the 27 nt ssDNA sequence was selected because of its slightly higher degree of $R_{ct}$ reduction and smaller standard error (Fig. 3a).

Another important aspect is the nature of the reporter sequence, once some previous studies have shown that Cas12a enzyme has no or minimal trans-cleavage activity towards dsDNA substrate (Chen et al., 2018). However, recent evidences showed that certain Cas12a variants, specially LbCas12a, had a notable dsDNA trans-degradation activity (Li et al., 2018; Mohammad et al., 2023; Smith et al., 2020, 2021). By maintaining the length of the DNA reporter constant, two different conditions were tested: a ssDNA and a dsDNA reporter (Fig. S7). For the dsDNA reporter, a complementary sequence of the ssDNA reporter was hybridized before its immobilization on the electrode surface to guarantee that all immobilized reporter sequences were dsDNA. It can be seen in Fig. 3b that when a dsDNA target is used, the trans-cleavage activity of Cas12a remains unaffected by the nature of the DNA reporter (single-stranded or double-stranded), and the same efficiency is observed for both systems. This result suggests that the recognition of dsDNA targets and further trans-cleavage ability has no relation with the nature of the DNA reporter, and the LbCas12a enzyme can cleave both ds- and ss-sequences with the same efficiency. However, when a ssDNA target is used, a lower trans-cleavage activity is observed for the dsDNA reporter, indicating a potential selectivity of Cas12a for the ssDNA reporter. This finding adds an interesting layer of complexity to the interaction between LbCas12a and its reporter molecules, suggesting that LbCas12a may have a preference for ssDNA reporters when encountering ssDNA targets, due to the specific binding, recognition properties, and steric hindrance of Cas12a. It is important to note, that even if a decrease in efficiency was observed for the dsDNA reporter when using a ssDNA target, the overall efficiency of the ssDNA target-activated systems was lower than for the dsDNA targets, confirming that the CRISPR/Cas12a system has a higher sensitivity for dsDNA targets, as already reporter in previous studies. Furthermore, the observed selectivity could potentially be harnessed for the discrimination of target DNA molecules based on their ss- or ds-nature, enabling the development of biosensors that can differentiate between different types of DNA targets. Considering the higher cleavage efficiency for ssDNA reporter sequences for both target scenarios, these sequences were chosen for further experiments.

### 3.4. Analytical performance of the label-free CRISPR-based biosensor

#### 3.4.1. Sensitivity and specificity

To evaluate the analytical performance of the electrochemical biosensor, the sensitivity of the proposed system was investigated for quantitative detection of target DNA under optimized experimental conditions. As previously discussed, two different scenarios were tested: a ssDNA and a dsDNA target. As observed in Fig. 4a, the percentage of $R_{ct}$ reduction increases with the increment of the target concentration. For the dsDNA target, the concentration was varied from 10 aM to 20 nM (Fig. S8) and, as shown in the inset of Fig. 4a, the $R_{ct}$ reduction had a strong linear relationship with the logarithmic concentration of dsDNA from 50 aM to 100 pM, with a linear equation: $\Delta R_{ct}/R_{ct0}$ (%) = 1.53 $\log C_{dsDNA}$ + 26.8 (M); ($R^2$ = 0.995, n ≥ 3). The obtained limits of detection (LOD) and quantification (LOQ) were 20 aM and 66 aM, for the dsDNA-triggered system, respectively. The LOD was calculated using the 3:1 S/N (signal-to-noise) ratio method and the LOQ value was considered as 3.3 times the LOD (Wan et al., 2016). In contrast to the dsDNA target, the ssDNA target showed a linear relationship between the percentage of $R_{ct}$ reduction and the target concentration, with two linear regions (Fig. S10). The first one, from 0.1 pM to 1 pM, presented the linear equation: $\Delta R_{ct}/R_{ct0}$ (%) = 6.17 $C_{ssDNA}$ + 0.865 (pM); ($R^2$ = 0.955; n ≥ 3) and the second, with a broader range from 10 pM to 1 nM, the equation: $\Delta Rct/Rct_0$ (%) = 0.0053 $C_{ssDNA}$ + 7.10 (pM); ($R^2$ = 0.988; n ≥ 3). The LOD for the ssDNA target sequence was 56 fM and the LOQ 185 fM. By comparing the two obtained LODs, a huge difference in the detection sensitivity can be observed. The dsDNA-triggered system showed 2800 times lower LOD in comparison to the ssDNA target, which indicates a preference of the CRISPR/Cas12a system for dsDNA sequences. These results corroborate previous studies that have shown that the catalytic efficiency of the trans-cleavage activity of Cas12a enzymes increases with the bonding of a dsDNA target (Chen et al., 2018; Li et al., 2018). This suggests that the NTS of the dsDNA activator helps stabilize the Cas12a complex in an optimal conformation for trans-cleavage, in which the PAM sequence may also account for higher efficiency.

Compared to conventional PCR-based detection methods, our approach offers significant advantages in terms of speed and ease of use. While PCR requires thermal cycling and typically takes several hours for completion, our method enables detection within 1 h at a constant temperature and without any pre-amplification step, eliminating the need for sophisticated equipment. Moreover, in contrast to other CRISPR-based electrochemical detection platforms (Table S2), which often require multiple detection steps and complex preparation, our proposed system shows remarkable advantages, with one of the lowest LOD and a wide linear range, better than most recently reported methods. Our biosensor could reach as low as 50 aM of target dsDNA without any pre-amplification step (Fig. S8), with the lowest achieved LOD for a CRISPR-based label-free electrochemical biosensor reported so far. Among other methods with lower LODs, the authors combined recombinase-assisted amplification (RAA) to a CRISPR/Cas12a system for *L. monocytogenes* detection (Zheng et al., 2023) or used a target-activated CRISPR/Cas14a system coupled with PtPd@PCN-224 nanoenzymes to amplify the signal for *Burkholderia pseudomallei*

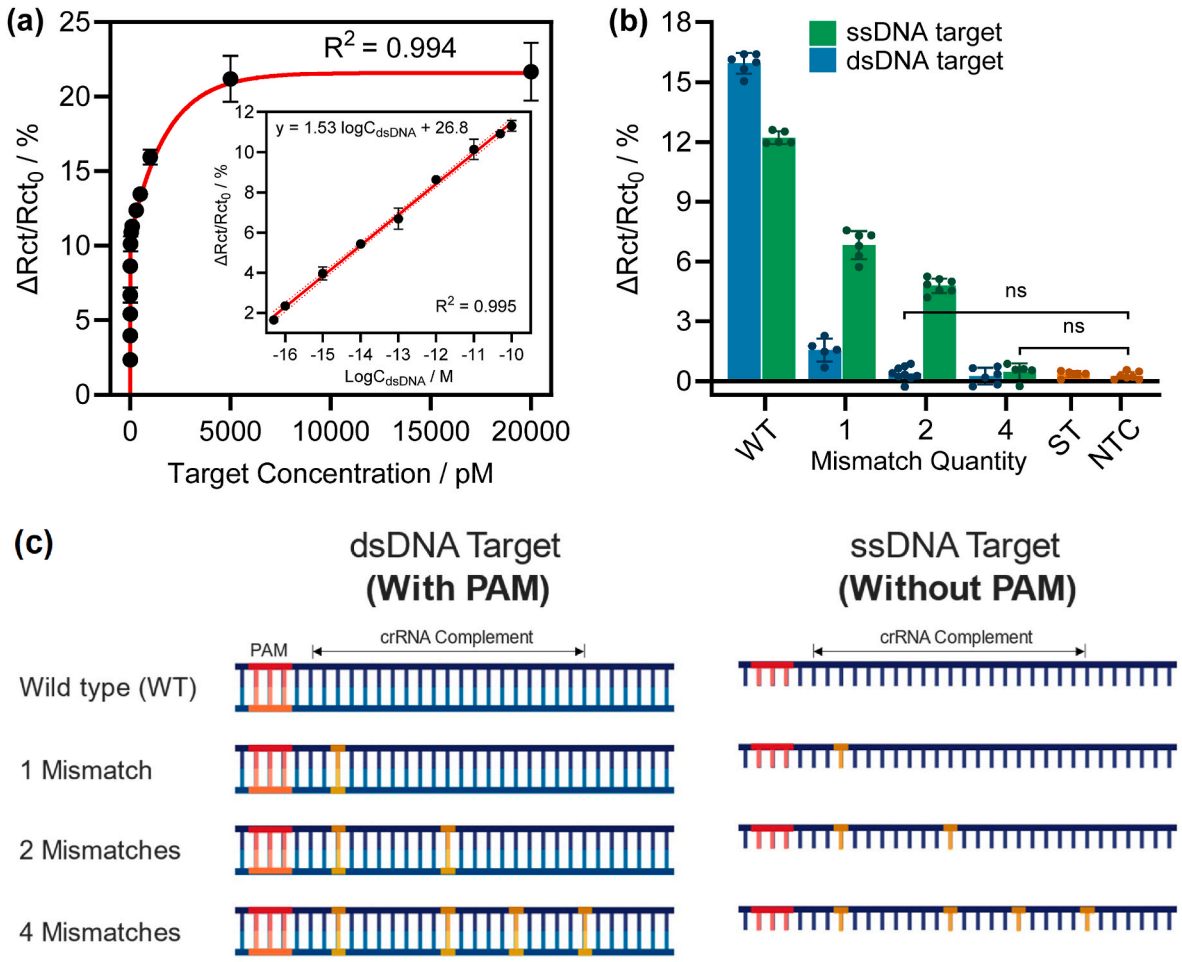



**Fig. 4.** **(a)** The relationship of the percentage of $R_{ct}$ reduction with the concentration of dsDNA target in the range of 50 aM to 20 nM. The inset shows the linear relationship between the percentage of $R_{ct}$ reduction and the logarithm of dsDNA target concentration ($R^2 = 0.995$); **(b)** Evaluation of the influence of different mismatches quantities on the percentage of $R_{ct}$ reduction for dsDNA and ssDNA targets. In all cases, 1 nM of DNA target sequence and 50 nM of Cas12a/crRNA duplex were used; **(c)** Schematic representation of the target strands (ssDNA and dsDNA) with different mismatches quantities (1, 2 and 4 mismatches), including PAM region and crRNA complement. The mismatches are highlighted in yellow. All data are expressed as mean ± standard deviation for $n \geq 5$ replicates. Statistical significance was analyzed using a two-tailed *t*-test: where ns = not significant with $\rho > 0.05$. Abbreviations: WT, wild type; ST, scrambled target; NTC, non-targeting control. (For interpretation of the references to colour in this figure legend, the reader is referred to the Web version of this article.)

bacteria detection (Li et al., 2023), adding extra complexity to the biosensor.

The remarkable level of ultra-sensitivity for our biosensor can be attributed to various aspects. Firstly, we employed EIS, which offers several advantages over other CRISPR-based electrochemical sensors. Specifically, EIS provides a more cost-effective and simpler approach compared to other techniques, while delivering superior sensitivity (Lazanas and Prodromidis, 2023). These sensors can outperform labelled-sensors based on pulse voltammetry, as impedance measurements can detect subtle changes in surface electrochemical properties, such as those caused by the trans-cleavage of the reporter probes. Second, in our work we used the Alt-R™ crRNAs (IDT, Iowa, USA), which present proprietary chemical modifications to protect the crRNA from degradation by RNases and to improve on-target cleavage efficiency. As shown in Fig. S11, when a crRNA without Alt-R™ modifications was tested under the same optimized reaction conditions and across three different concentrations of ssDNA target, a clear difference in trans-cleavage activity was observed. Specifically, the Alt-R™ crRNAs demonstrated an average 1.3-fold enhancement in signal output after trans-cleavage, indicating improved cleavage efficiency and detection capability. Furthermore, by comparing previous works, our approach benefits from careful optimization of reaction conditions, such as buffer composition and reporter immobilization. Some articles employ unoptimized buffers concentration for the CRISPR reaction and measurement, which can lead to lower trans-cleavage activities and, consequently, impaired sensitivity (Bonini et al., 2021; Liu et al., 2022, 2024). We also fine-tuned the reporter probe conditions, including its length and concentration, which are critical factors for maximizing performance in label-free detection. Furthermore, our study utilizes a TA-rich reporter sequence (85 %), which has been demonstrated to exhibit higher trans-cleavage rate compared to GC-rich sequences (Nguyen et al., 2020).

Further considering the application of the biosensor in clinical settings, especially for the detection of bacteria-caused blood-stream infection (BSI), our system shows a practical utility. Several studies have demonstrated that bacterial load correlates with disease severity and is predictive of patient's illness state. In subjects with suspected or confirmed bloodstream infections, the amount of bacterial nucleic acid ranges from $10^6$ to $10^7$ genome copies/L, being a bacterial load of $10^6$ genome copies/L a critical threshold above which patients had an increased risk of developing septic shock (Bacconi et al., 2014; Kirkbright et al., 2011; Opota et al., 2015). Our system was able to detect 320 DNA copies/L for the dsDNA target and 17000 DNA copies/L for the ssDNA target, which is at least 60 times lower than the critical value for sepsis identification. As seen, in both scenarios our developed biosensor achieved a detection value of pathogenic bacteria that could indicate an

early diagnosis of sepsis, further preventing complications and treatment costs.

The specificity and the influence of the PAM sequence on the detection capability was tested next. We systematically introduced nucleotide mismatches to the target and complementary strands (Fig. 4c), and evaluated four different conditions by varying the mismatch quantity: one mismatch in the PAM-adjacent "seed region", two mismatches, four mismatches, and a scrambled target, which presented the correct target nucleic acid composition but in an random way. The same previous mismatches were maintained for increased mismatch quantity, and changes were made in both target sequences. As seen in Fig. 4b, all mismatches in target sequence decreased the trans-cleavage efficiency, resulting in lower $R_{ct}$ reduction. The scrambled target showed no trans-cleavage activity, as well as the NTC. Furthermore, by analyzing the mismatch quantity, it becomes clear that altering just one nucleotide in the original target DNA sequence drastically reduces cleavage activity for both targets, with the mismatch in the PAM-adjacent "seed region" almost inhibiting the trans-cleavage only for the dsDNA activator. Even considering that some Cas12a activity remains detectable, this residual trans-cleavage disappears when the target sequence is altered by 2 or 4 nucleotides, showing that the system is highly specific for the original, unmutated sequence. Conversely, in the PAM-independent system, only the sequence with 4 altered nucleotides shows no trans-cleavage activity. Sequences with 1 or 2 mismatches exhibit some trans-cleavage, but at a much lower magnitude than the original ssDNA sequence. These results reinforce that the Cas12a enzyme better discriminates mismatches in dsDNA targets when compared to ssDNA targets, and is less likely to tolerate mutations in dsDNA targets. It also confirms that PAM-mediated binding of dsDNA is crucial for base pairing between the crRNA and the target strand. This mechanism ensures that the Cas protein selectively binds to the correct target sequence, minimizing off-target effects and accurately triggering the collateral activity. As a result, this process enhances both the specificity and sensitivity of the biosensor.

### 3.4.2. *Stability and successive cleavage*

Stability experiments were conducted through storing the prepared electrodes in Tris buffer (10 mM Tris-HCl, 100 mM NaCl, 10 mM $MgCl_2$, pH 7.4) at 4 °C for 5 days. $R_{ct}$ was measured every single day to evaluate the long-term storage stability. Over 85 % of the initial $R_{ct}$ value remained after 5 days of storage (Fig. 5a). Even considering a decrease in $R_{ct}$, possibly related to the detachment of some ssDNA reporter molecules from the electrode surface; on the fifth day, a CRISPR/Cas12a reaction with ssDNA target (1 nM) was conducted to confirm that the electrodes could still be used. After 5 days of storage, the same cleavage activity was observed for the previously prepared electrodes, indicating that the system was working properly and could be still used after this period.

By considering the applicability of the bioassay for consecutive detection steps, successive cleavage cycles over the same modified electrode were evaluated. The results shown in Fig. 5b prove that the same electrode could be used for at least 6 successive cleavage cycles

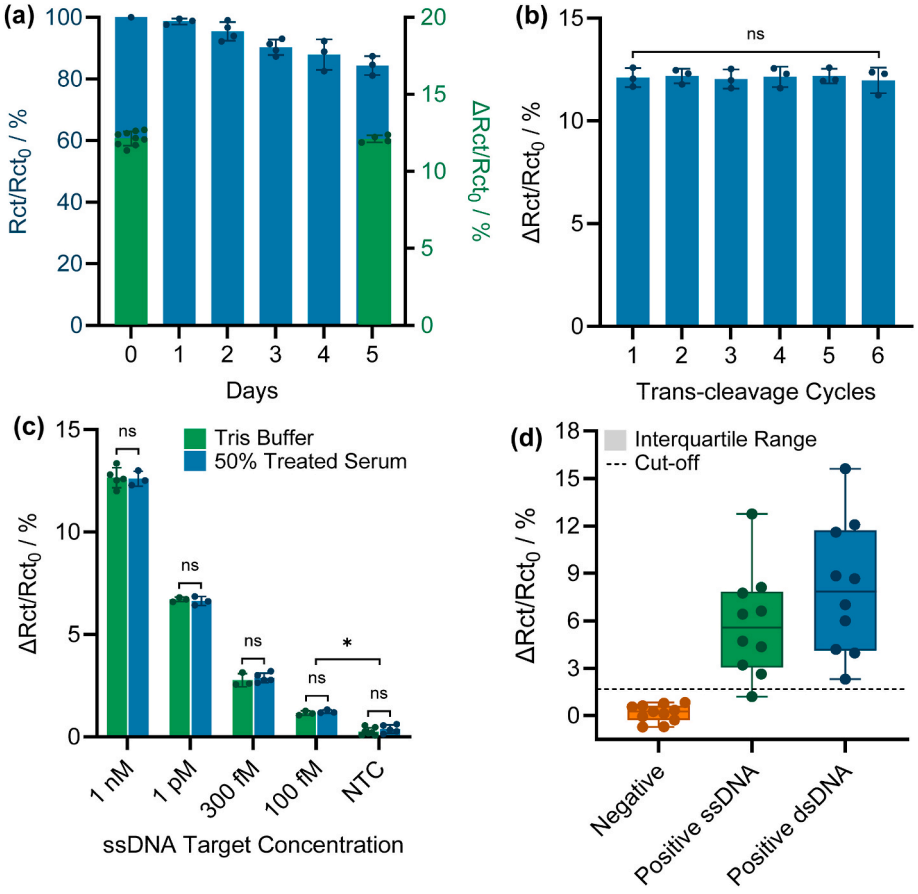



**Fig. 5.** **(a)** Stability of the prepared biosensor maintained at 4 °C and the percentage of $R_{ct}$ reduction after five days; **(b)** Comparison of six successive trans-cleavage steps on the same electrode (1 nM of ssDNA target); **(c)** Comparison of the biosensor response for four different ssDNA target concentrations (100 fM, 300 fM, 1 pM and 1 nM) and NTC in Tris buffer (10 mM Tris-HCl, 100 mM NaCl, 10 mM $MgCl_2$, pH 8.0) and 50 % treated human serum. Data are expressed as mean ± standard deviation for $n \geq 3$ replicates; **(d)** Statistical analysis of the percentage of $R_{ct}$ reduction for the biosensor in the detection of positive DNA targets in 50 % treated human serum. Statistical significance was analyzed using a two-tailed *t*-test: where ns = not significant with $\rho > 0.05$, and the asterisk (*) denotes significant differences with $\rho < 0.05$.

when using the same concentration of ssDNA target (1 nM). It was observed that the same percentage of $R_{ct}$ reduction was achieved for each cleavage round. This result reinforces the simplicity and practicality of the proposed biosensor for rapid detection of bacterial DNA.

### 3.4.3. Serum sample analysis

To investigate the potential application of the proposed biosensor in detecting pathogenic bacterial DNA in clinical samples, we employ it to detect ssDNA and dsDNA targets in human serum. As the serum is a very complex sample, which may contain interference components, especially for CRISPR-based assay, we followed a well-established protocol for pre-treatment and DNA extraction (SI). Once several studies have already established the relevance of detection pathogenic cell-free DNA in serum for bloodstream infections diagnosis (Eichenberger et al., 2021; Guimaraes et al., 2019), different concentrations of target DNA were spiked into serum samples, followed by DNA extraction steps and diluted 2 × with Tris buffer (10 mM Tris-HCl, 100 mM NaCl, 10 mM $MgCl_2$, pH 8.0). The results comparing the detection of cell-free ssDNA spiked into 50 % serum samples and in 100 % Tris buffer (10 mM Tris-HCl, 100 mM NaCl, 10 mM $MgCl_2$, pH 8.0) are shown in Fig. 5c. The obtained recoveries values for different spiked target concentrations were 107 %, 94.6 %, 106 % and 111 % for 1 nM, 1 pM, 300 fM and 100 fM, respectively. It is important to note that the NTC produced the same result in both media, confirming that the assay has good accuracy to detect DNA targets in serum samples, without any observed matrix or interference effect. Additionally, we evaluated the specificity of the biosensor in detecting different spiked pathogenic bacterial DNAs. As shown in Fig. S13, the presence of non-target pathogenic bacterial DNAs did not activate the CRISPR/Cas12a system, and no change in signal was observed, even at a high ssDNA target concentration (1 nM). However, when a mixture containing all non-target DNAs along with the *S. aureus* target DNA (100 pM) was tested, the same cleavage activity as observed with the *S. aureus* target alone was recorded. This indicates that the biosensor exhibits high specificity for detecting *S. aureus* DNA in clinical samples, even in the presence of other bacteremia-causing pathogens.

Following this analysis, 31 simulated serum samples (11 negative, 10 ssDNA positive and 10 dsDNA positive) were tested in a concentration range compatible with the calibration curve. The $\Delta R_{ct}/R_{ct0}$ value increased significantly for positive samples, indicating the collateral activity on the reporter sequences. The $R_{ct}$ values obtained for positive/negative samples were submitted to statistical analysis and Fig. 5d shows the change in $R_{ct}$ for different analyzed samples. The proposed method was able to separate both positive cases from the negatives. To discriminate the results, an optimal cut-off value (positive/negative threshold) of 1.80 % was calculated based on the test results from negative samples by adding the average ($\bar{x}$) of negative individual samples response by 3 × their standard deviation (cut-off = $\bar{x} + 3 \times SD$). Only one ssDNA positive sample (100 fM) was misclassified as a negative case and all classified positive samples simulated real positive cases, showing no false positive results. By considering all the samples, a receiver operating characteristic (ROC) curve was constructed in order to determine the accuracy of the test, showing an area under the curve (AUC) of 0.968 (Fig. S14). The proposed CRISPR-based electrochemical biosensor achieved a specificity of 95 %, a sensitivity of 100 % and an accuracy of 96.8 %, clearly demonstrating its potential in the accurate and sensitive detection and discrimination of bacterial DNA in human serum for sepsis diagnosis.

## 4. Conclusions

Herein, we successfully demonstrated the application of a label-free impedimetric biosensor coupled with a CRISPR/Cas12a system for *Staphylococcus aureus* detection. The detection mechanism relies on the trans-cleavage of DNA reporters immobilized onto gold electrodes upon target recognition by the Cas12a/crRNA complex, which causes a reduction in the $R_{ct}$ between the electrode surface and a redox probe in the electrolyte. The biosensor was optimized for DNA reporter immobilization and CRISPR/Cas12a reaction conditions. The trans-cleavage of the reporter sequences was evaluated upon recognition of ssDNA and PAM-containing dsDNA targets by the RNP complex. The results indicate that when the CRISPR/Cas12a duplex recognizes the dsDNA target, the nature of the DNA reporter does not influence the trans-cleavage efficiency. However, when a ssDNA target activates the system, a lower trans-cleavage activity is observed for the dsDNA reporter, suggesting an additional selectivity of Cas12a. For the dsDNA triggered system, an ultra-low limit of detection of 20 aM was obtained without any pre-amplification steps, in addition to the ability to discriminate a single-nucleotide mismatch. In spiked serum samples, this biosensor demonstrated exceptional sensitivity, specificity, and accuracy, evidencing its potential as an alternative detection method for sepsis diagnosis. While this system shows great potential for the early detection of pathogenic bacterium, it should be further adapted to miniaturized electrodes and portable devices to ensure proper performance in POC settings. Furthermore, the proposed method should be adapted for the detection of other pathogens by rationally redesigning the crRNA, enabling the development of more versatile and simple detection tools.

## CRediT authorship contribution statement

**Dagwin Wachholz Junior:** Writing – review & editing, Writing – original draft, Visualization, Validation, Methodology, Investigation, Formal analysis, Data curation, Conceptualization. **Rafael Gonçalves Pontes:** Writing – review & editing, Writing – original draft, Formal analysis. **Bruna M. Hryniewicz:** Writing – review & editing, Writing – original draft, Formal analysis. **Lauro Tatsuo Kubota:** Supervision, Resources, Project administration, Funding acquisition, Conceptualization.

## Funding sources

This research was funded by The São Paulo Research Foundation (FAPESP: 2014/50867–3, 2013/22127–2 and 2019/00166-2), National Institute of Science & Technology in Bioanalytic (INCTBio, INCT-MCTI/CNPq/CAPES/FAPs n° 16/2014), Coordination for the Improvement of Higher Education Personnel (CAPES), and National Council for Scientific and Technological Development (CNPq) (Projects: 136386/2019-9, 434303/2016–0 and MCTIC/CNPq/FNDCT/MS/SCTIE/Decit n° 07/2020). DWJ acknowledges FAPESP and CAPES for the doctoral fellowship (Process: 2021/09706–0 (FAPESP); Process: 88887.645260/2021–00 (CAPES)). RGP acknowledges CNPq (Grant 160903/2021-1). BMH acknowledges FAPESP (Process: 2023/09451-7).

## Declaration of competing interest

The authors declare that they have no known competing financial interests or personal relationships that could have appeared to influence the work reported in this paper.

## Acknowledgments

This paper is dedicated to the memory of Professor Lauro Tatsuo Kubota, who recently passed away. We would like to express our deepest gratitude to his mentorship and friendship. Professor Kubota was more than a supervisor; he was a steadfast supporter, always willing to share his extensive knowledge, provide encouragement, and inspire those around him. This work is the result of his scientific pioneering and his forefront contributions to Brazilian science. We are grateful for all the opportunities and invaluable guidance you provided, Professor Lauro! Your dedication and passion for science will continue to inspire us. The authors also thank Professor Saimon Moraes Silva for the review of this paper.

## Appendix A. Supplementary data

Supplementary data to this article can be found online at https://doi.org/10.1016/j.bios.2025.117607.

## Data availability

Data will be made available on request.

## References

Bacconi, A., et al., 2014. J. Clin. Microbiol. 52, 3164–3174. https://doi.org/10.1128/jcm.00801-14.
Barrangou, R., et al., 2007. Science 315, 1709–1712. https://doi.org/10.1126/science.1138140.
Bloos, F., Mancini, N. (Eds.), 2015. Sepsis: Diagnostic Methods and Protocols. Springer, New York, New York, NY, pp. 247–260. https://doi.org/10.1007/978-1-4939-1776-1_19.
Bonini, A., et al., 2021. J. Pharmaceut. Biomed. Anal. 204, 114268. https://doi.org/10.1016/j.jpba.2021.114268.
Caliendo, A.M., et al., 2013. Clin. Infect. Dis. 57, S139–S170. https://doi.org/10.1093/cid/cit578.
Chakraborty, J., et al., 2022. ACS Omega 7, 39562–39573. https://doi.org/10.1021/acsomega.2c04513.
Chen, J.S., Doudna, J.A., 2017. Nat. Rev. Chem 1, 78. https://doi.org/10.1038/s41570-017-0078.
Chen, J.S., et al., 2018. Science 360, 436–439. https://doi.org/10.1126/science.aar6245.
da Silva, E.T.S.G., et al., 2017. Chemelectrochem 4, 778–794. https://doi.org/10.1002/celc.201600758.
Dai, Y., Liu, C.C., 2019. Angew. Chem. Int. Ed. 58, 12355–12368. https://doi.org/10.1002/anie.201901879.
Deroco, P.B., et al., 2021. Sensor. Actuator. B Chem. 349, 130821. https://doi.org/10.1016/j.snb.2021.130821.
Deroco, P.B., , et al.Kubota, L.T., et al. (Ed.), 2022. Tools and Trends in Bioanalytical Chemistry. Springer International Publishing, Cham, pp. 543–558. https://doi.org/10.1007/978-3-030-82381-8_27.
Deroco, P.B., et al., 2023. Electroanalysis 35, e202200177. https://doi.org/10.1002/elan.202200177.
Drain, P.K., et al., 2014. Lancet Infect. Dis. 14, 239–249. https://doi.org/10.1016/S1473-3099(13)70250-0.
Eichenberger, E.M., et al., 2021. Clin. Infect. Dis. 74, 2020–2027. https://doi.org/10.1093/cid/ciab742.
Gootenberg, J.S., et al., 2018. Science 360, 439–444. https://doi.org/10.1126/science.aaq0179.
Guimaraes, A.O., et al., 2019. Open Forum Infect. Dis. 6, ofz126. https://doi.org/10.1093/ofid/ofz126.
Ikuta, K.S., et al., 2022. Lancet 400, 2221–2248. https://doi.org/10.1016/S0140-6736(22)02185-7.
Jinek, M., et al., 2012. Science 337, 816–821. https://doi.org/10.1126/science.1225829.
Kabay, G., et al., 2022. Adv. Mater. 34, 2201085. https://doi.org/10.1002/adma.202201085.
Kaminski, M.M., et al., 2021. Nat. Biomed. Eng. 5, 643–656. https://doi.org/10.1038/s41551-021-00760-7.
Kirkbright, S., et al., 2011. Emerg. Med. Australasia (EMA) 23, 502–506. https://doi.org/10.1111/j.1742-6723.2011.01445.x.
Lazanas, A.C., Prodromidis, M.I., 2023. ACS Meas. Sci. Au 3, 162–193. https://doi.org/10.1021/acsmeasuresciau.2c00070.
Li, C., et al., 2023. Biosens. Bioelectron. 225, 115098. https://doi.org/10.1016/j.bios.2023.115098.
Li, S.-Y., et al., 2018. Cell Res. 28, 491–493. https://doi.org/10.1038/s41422-018-0022-x.
Li, Y., et al., 2019. Trends Biotechnol. 37, 730–743. https://doi.org/10.1016/j.tibtech.2018.12.005.
Liu, B., et al., 2024. Sensor. Actuator. B Chem. 406, 135406. https://doi.org/10.1016/j.snb.2024.135406.
Liu, N., et al., 2022. Bioelectrochemistry 146, 108105. https://doi.org/10.1016/j.bioelechem.2022.108105.
Mancini, N., et al., 2010. Clin. Microbiol. Rev. 23, 235–251. https://doi.org/10.1128/cmr.00043-09.
Mohammad, N., et al., 2023. Nucleic Acids Res. 51, 9894–9904. https://doi.org/10.1093/nar/gkad715.
Nguyen, L.T., et al., 2020. Nat. Commun. 11, 4906. https://doi.org/10.1038/s41467-020-18615-1.
Opota, O., et al., 2015. Clin. Microbiol. Infection 21, 323–331. https://doi.org/10.1016/j.cmi.2015.02.005.
Panicker, L.R., et al., 2024. Bioelectrochemistry 156, 108594. https://doi.org/10.1016/j.bioelechem.2023.108594.
Pliakos, E.E., et al., 2018. Clin. Microbiol. Rev. 31. https://doi.org/10.1128/cmr.00095-17 doi:10.1128/cmr.00095-17.
Rahn, K.L., et al., 2023. Annu. Rev. Anal. Chem. 16, 49–69. https://doi.org/10.1146/annurev-anchem-091622-085754.
Shi, R., et al., 2024. TrAC, Trends Anal. Chem. 177, 117796. https://doi.org/10.1016/j.trac.2024.117796.
Smith, C.W., et al., 2021. ACS Synth. Biol. 10, 1785–1791. https://doi.org/10.1021/acssynbio.1c00204.
Smith, C.W., et al., 2020. Biochemistry 59, 1474–1481. https://doi.org/10.1021/acs.biochem.0c00140.
Tang, Y., et al., 2021. Chem. Soc. Rev. 50, 11844–11869. https://doi.org/10.1039/D1CS00098E.
van Dongen, J.E., et al., 2020. Biosens. Bioelectron. 166, 112445. https://doi.org/10.1016/j.bios.2020.112445.
Vidic, J., Manzano, M., 2021. Curr. Opin. Electrochem. 29, 100750. https://doi.org/10.1016/j.coelec.2021.100750.
Wachholz Junior, D., Kubota, L.T., 2024. Talanta 278, 126467. https://doi.org/10.1016/j.talanta.2024.126467.
Wan, J., et al., 2016. Sci. Rep. 6, 19806. https://doi.org/10.1038/srep19806.
Wu, J., et al., 2023. Nat. Rev. Bioeng. 1, 346–360. https://doi.org/10.1038/s44222-023-00032-w.
Zasowski, E.J., et al., 2016. Clin. Infect. Dis. 62, 1242–1250. https://doi.org/10.1093/cid/ciw110.
Zhang, X., et al., 2022. Small Methods 6, 2200794. https://doi.org/10.1002/smtd.202200794.
Zheng, S., et al., 2023. Food Control 146, 109528. https://doi.org/10.1016/j.foodcont.2022.109528.